

P325

Continuous Reservoir Monitoring with Asynchronous Simultaneous-source Seismic Data

G. Ayeni* (Stanford University) & B. Biondi (Stanford University)

SUMMARY

We propose the use of asynchronous simultaneous-source seismic data for continuous reservoir monitoring.

By acquiring data from multiple asynchronous seismic sources at short time intervals, we can capture short-period variations in reservoir properties.

Instead of separating the data sets into independent shot records, we propose direct imaging using a regularized joint least-squares migration/inversion approach.

Least-squares migration/inversion attenuates artifacts that are caused by discrepancies in the recorded data sets.

Using a modified 2D Marmousi model, we show that our method gives time-lapse image volumes of comparable quality to migrated single-source data sets.

Introduction

Reservoirs can be *continuously* monitored using asynchronous simultaneous-source seismic data sets. Simultaneous-source acquisition involves recording data from more than one seismic source at a time (Hampson et al., 2008). Typically, the recorded *multiplexed* data are separated into independent shot components, which are then processed using standard methods (Spitz et al., 2008). Previous authors have shown that production-scale simultaneous-source acquisition is feasible and that it lowers both the acquisition cost and the acquisition time-window (Howe et al., 2009).

Although seismic reservoir monitoring is a well-developed technology, several limitations exist. Because the cost of conventional (single-source) acquisition is high, it is impractical to acquire seismic data sets at short time intervals. Therefore, typical monitoring survey intervals may be too large to measure production-related, short-period variations in reservoir properties. Furthermore, limited acquisition windows in emerging frontiers (e.g., the Arctic) provide a potential acquisition challenge. By acquiring time-lapse data sets with multiple, relatively cheap seismic sources, we can limit the acquisition time and cost, and acquire more data sets at shorter time intervals. Sufficiently small survey intervals will enable *quasi-continuous* monitoring of changes in reservoir properties. Quasi-continuous monitoring may also be achieved by sparse data recording followed by interpolation (Arogunmati and Harris, 2009).

Depending on operational limitations, an arbitrary number of seismic sources can be used for each survey. Instead of separating the recorded data sets into independent shots, they should be processed directly. Discrepancies between these data sets are of two forms, namely, geometry and relative shot-timing non-repeatabilities (Ayeni et al., 2009). Although modern acquisition techniques can improve repeatability of shot-receiver positions, field conditions usually prevent perfect repeatability. Furthermore, because we assume asynchronous shooting, the relative time-lags between sources differ between surveys. Because conventional time-lapse seismic processing methods are insufficient to attenuate artifacts caused by these non-repeatability sources, we propose a least-squares migration/inversion solution.

Using a joint least-squares formulation, we directly invert multiple simultaneous-source data sets. Because the data sets are inverted directly, we combine the cost-saving advantages of both simultaneous-source acquisition and phase encoding migration (Romero et al., 2000). By including structural and temporal constraints in the inversion, we obtain geologically plausible time-lapse seismic images. We assume that the velocity and structural dips are known and that they change slowly between surveys. In addition, we assume that for each survey, the shot-receiver positions and relative shot timings are known.

In this paper, we first summarize continuous monitoring with asynchronous simultaneous-source data. Then, we discuss regularized joint inversion of multiple simultaneous-source data sets. Finally, using a 2D numerical model, we show that our method is realistic for continuous reservoir monitoring.

Method

Asynchronous simultaneous-source acquisition can be represented as a linear combination of phase-shifted shots. The data d recorded at receiver r due to shots starting from $s = q$ to $s = p$ is given by

$$d(\mathbf{x}_{\text{spq}}, \mathbf{x}_r, \omega) = \sum_{s=p}^q a(\gamma_s) \omega^2 \sum_{\mathbf{x}} f_s(\omega) G(\mathbf{x}_s, \mathbf{x}, \omega) G(\mathbf{x}, \mathbf{x}_r, \omega) m(\mathbf{x}), \quad (1)$$

where ω is frequency, $m(\mathbf{x})$ is the reflectivity at image points \mathbf{x} , f_s is the source wavelet, and $G(\mathbf{x}_s, \mathbf{x}, \omega)$ and $G(\mathbf{x}, \mathbf{x}_r, \omega)$ are respectively the Green's functions from \mathbf{x}_s to \mathbf{x} and from \mathbf{x} to \mathbf{x}_r . The encoding function $a(\gamma_s)$ is given by

$$a(\gamma_s) = e^{i\gamma_s} = e^{i\omega t_s}, \quad (2)$$

where γ_s , the time-delay function, depends on the delay time t_s at shot s .

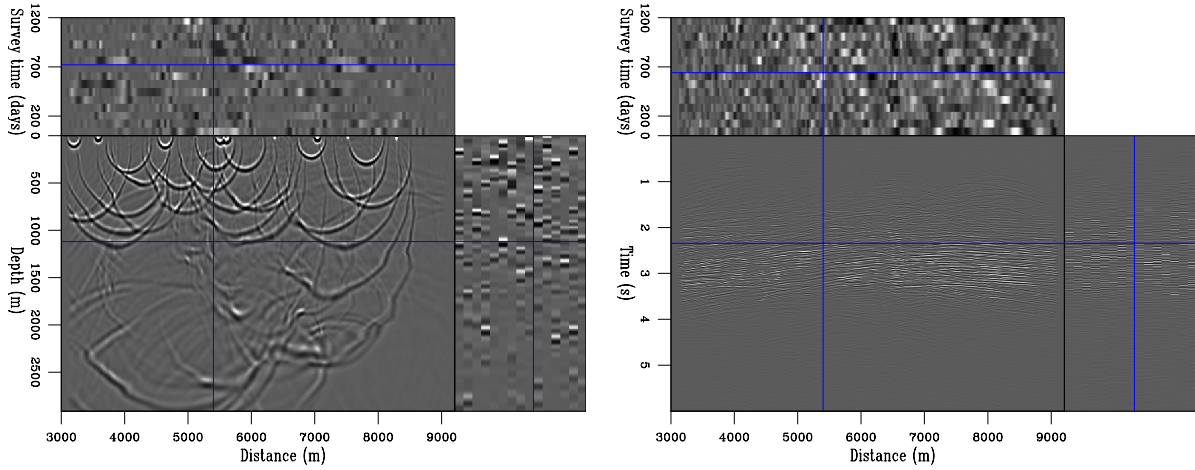


Figure 1 Wavefields (left) and synthetic data (right) from multiple asynchronous sources. Note that the third dimension denotes survey/recording time.

For efficiency of the proposed method, no attempt is made at repeating either the geometry or relative shot timings for different surveys. Therefore, the recorded data for any survey have unique distributions of \mathbf{x}_s , \mathbf{x}_r , and γ_s . Figure 1 shows example wavefields and recorded data from multiple asynchronous sources through a 2D-model. In both figures, the third dimension represents the survey time, while the orthogonal lines indicate positions of the shown slices within the cube.

For an arbitrary survey i , we can simplify the modeling equation into the form

$$\tilde{\mathbf{d}}_i = \mathbf{B}_i \mathbf{L}_i \mathbf{m}_i = \tilde{\mathbf{L}}_i \mathbf{m}_i, \quad (3)$$

where $\tilde{\mathbf{d}}$ is the recorded data, \mathbf{B} is the encoding operator, \mathbf{L} is the modeling operator, \mathbf{m} is the earth reflectivity, and $\tilde{\mathbf{L}} = \mathbf{B}\mathbf{L}$. The migrated image, computed by applying the adjoint operator $\tilde{\mathbf{L}}^T$ to $\tilde{\mathbf{d}}$, will contain cross-term artifacts generated by cross-correlation between incongruous source and wavefields (Romero et al., 2000; Tang and Biondi, 2009). Because of the associated geometry and relative shot-time non-repeatability, different data sets have unique cross-term artifacts. To attenuate these artifacts, for N surveys, we minimize a global cost function S given by

$$S(\mathbf{m}_0, \dots, \mathbf{m}_N) = \sum_{i=0}^N \left\| \tilde{\mathbf{L}}_i \mathbf{m}_i - \tilde{\mathbf{d}}_i \right\|^2 + \sum_{i=0}^N \left\| \epsilon_i \mathbf{R}_i \mathbf{m}_i \right\|^2 + \sum_{i=1}^N \left\| \zeta_i \mathbf{\Lambda}_i (\mathbf{m}_{i-1}, \mathbf{m}_i) \right\|^2, \quad (4)$$

where, the parameters ϵ_i and ζ determine the strengths of the spatial and temporal regularization operators, \mathbf{R} and $\mathbf{\Lambda}$ respectively. Because several shots are encoded and directly imaged, the computational cost of this approach is considerably reduced compared to non-encoded data sets. In this paper, the spatial regularization operator is a system of non-stationary dip-filters, whereas the temporal regularization operator is a gradient between surveys. We compute dips using the plane-wave destruction method (Fomel, 2002), and dip-filters using factorized directional Laplacians (Hale, 2007). Similar formulations have been applied to other time-lapse imaging problems (Ajo-Franklin et al., 2005).

Numerical Example

The proposed method was applied to a modified 2D Marmousi model (Figure 2). We neglect overburden geomechanical changes and assume no change in reflectivity, except within the reservoir (Figure 2). Using a Born modeling algorithm, we simulated 15 data sets representing different production stages. The data sets, each comprising 56 asynchronous shot records with unique shot positions and relative shot-timings, were migrated with a phase-encoding one-way wave-equation operator. We estimated the dip-field (Figure 2) from the migrated baseline image and we minimized the cost function (equation 4) with a conjugate gradient method. Figures 3 to 5 show the migrated and inverted image volumes.

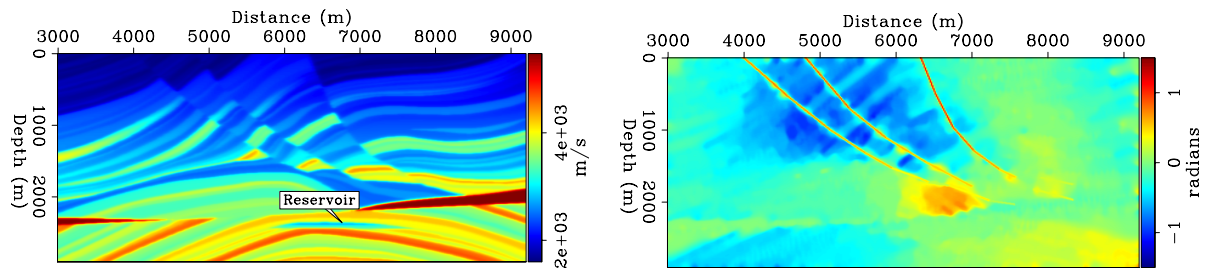


Figure 2 Baseline velocity model (left) and dip-field (right) computed from the migrated baseline image.

Discussion

If survey intervals are sufficiently small, time-lapse seismic can provide a continuous measure of reservoir property changes (Figure 3). For example, the top panel in Figure 3 shows a continuous measure of the spatial and temporal change in reflectivity at a constant depth. By using an asynchronous simultaneous-source acquisition approach, data required for continuous monitoring can be acquired at a fraction of the cost of conventional acquisition. Because the amount of recorded data is large, instead of separating them into independent shot records, they can be directly imaged with a phase-encoded migration operator. However, the associated geometry and shot-timing non-repeatabilities generate uncorrelated artifacts that contaminate the migrated time-lapse images (Figure 4). These artifacts can be attenuated by inverting the data sets using a regularized least-squares approach (Figure 5). The time-lapse image volume obtained by least-squares inversion (Figure 5) is of comparable quality to the volume obtained by migration of perfectly repeated single-source data (Figure 3).

Conclusions

Using asynchronous simultaneous-source acquisition, we can acquire short-interval seismic data sets. Joint least-squares migration/inversion of the recorded data sets gives good-quality images of reservoir property changes. Combining these acquisition and processing approaches provides a realistic framework for continuous reservoir monitoring. Although geomechanical and large velocity changes are not included in this analysis, they will be essential in most practical field applications.

Acknowledgements

We thank sponsors of the Stanford Exploration Project for their financial support.

References

- Ajo-Franklin, J.B., Urban, J. and Harris, J.M. [2005] Temporal integration of seismic traveltome tomography. *SEG Technical Program Expanded Abstracts*, **24**(1), 2468–2471, doi:10.1190/1.2148222.
- Arognmati, A. and Harris, J.M. [2009] An approach for quasi-continuous time-lapse seismic monitoring with sparse data. *SEG Technical Program Expanded Abstracts*, **28**(1), 3899–3903, doi:10.1190/1.3255682.
- Ayeni, G., Tang, Y. and Biondi, B. [2009] Joint preconditioned least-squares inversion of simultaneous source time-lapse seismic data sets. *SEG Technical Program Expanded Abstracts*, **28**(1), 3914–3918, doi:10.1190/1.3255685.
- Fomel, S. [2002] Applications of plane-wave destruction filters. *Geophysics*, **67**, 1946–1960.
- Hale, D. [2007] Local dip filtering with directional laplacians. *CWP Project Reiew*, **567**(1), 91–102.
- Hampson, G., Stefani, J. and Herkenhoff, F. [2008] Acquisition using simultaneous sources. *The Leading Edge*, **27**(7), 918–923, doi:10.1190/1.2954034.
- Howe, D. et al. [2009] Independent simultaneous sweeping in libya-full scale implementation and new developments. *SEG Technical Program Expanded Abstracts*, **28**(1), 109–111, doi:10.1190/1.3255044.
- Romero, L.A., Ghiglia, D.C., Ober, C.C. and Morton, S.A. [2000] Phase encoding of shot records in prestack migration. *Geophysics*, **65**(2), 426–436, doi:10.1190/1.1444737.
- Spitz, S., Hampson, G. and Pica, A. [2008] Simultaneous source separation: A prediction-subtraction approach. *SEG Technical Program Expanded Abstracts*, **27**(1), 2811–2815, doi:10.1190/1.3063929.
- Tang, Y. and Biondi, B. [2009] Least-squares migration/inversion of blended data. *SEG Technical Program Expanded Abstracts*, **28**(1), 2859–2863, doi:10.1190/1.3255444.

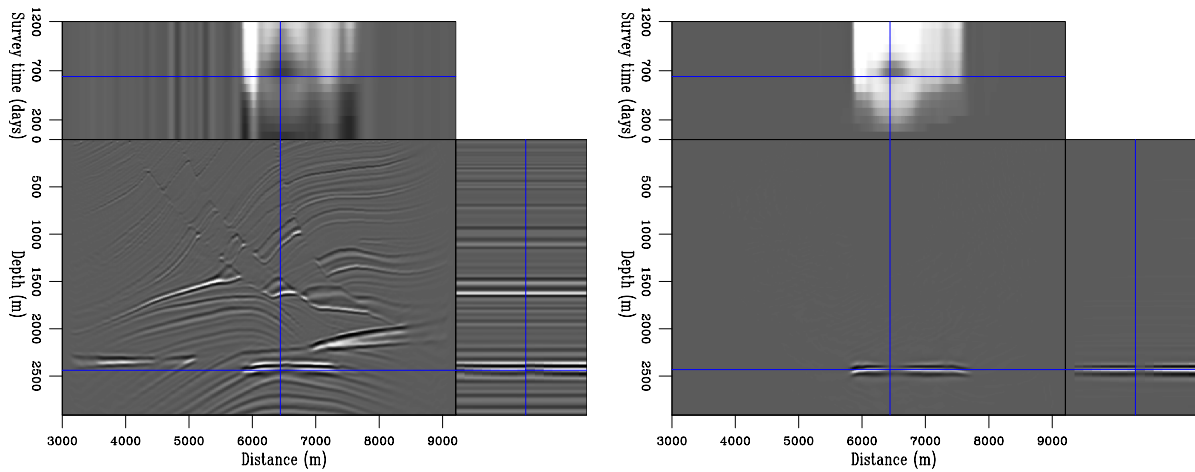


Figure 3 Migrated image volume (left) and corresponding time-lapse image volume (right) obtained from 15 perfectly repeated conventional (single-source) data sets. Note that the three orthogonal slices show the spatial and temporal change in reflectivity.

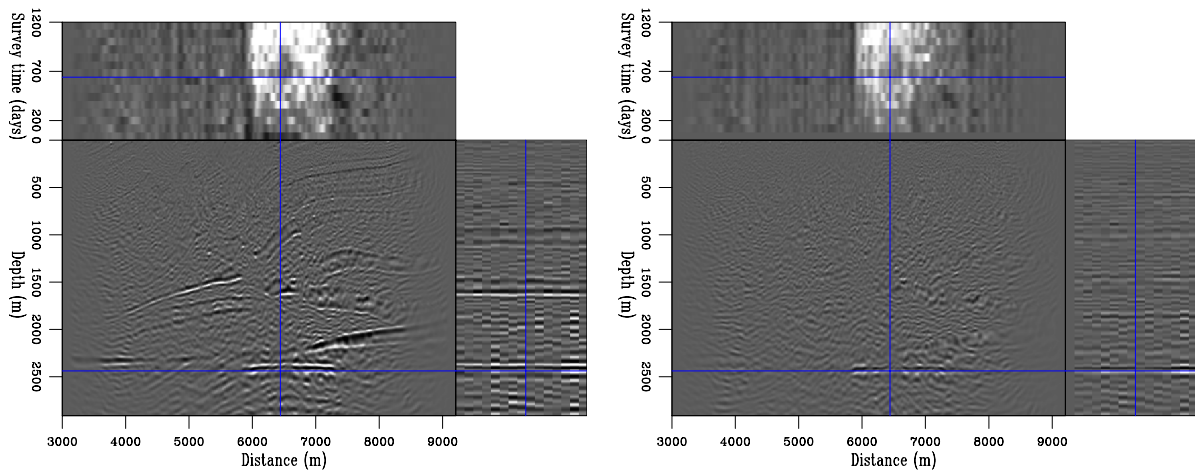


Figure 4 Migrated image volume (left) and corresponding time-lapse image volume (right) obtained from 15 asynchronous simultaneous-source data sets. Note that non-correlated artifacts degrade the image volumes.

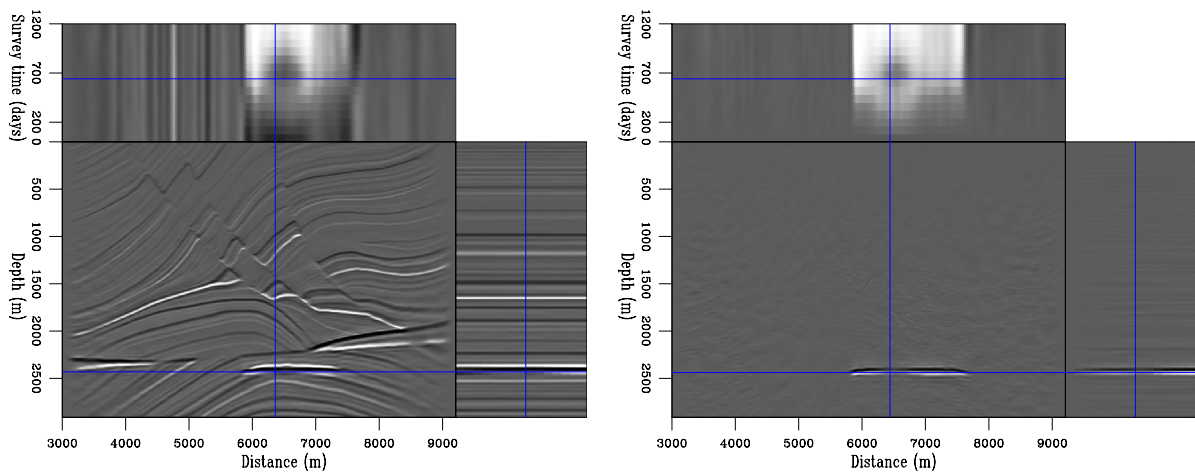


Figure 5 Inverted image volume (left) and corresponding time-lapse image volume (right) obtained from 15 asynchronous simultaneous-source data sets. Note that inversion has attenuated the non-correlated artifacts (Figure 4), thereby improving the image quality.